

CARBON NANOWALLS AS SUITABLE LAYERS FOR LUBRICITY IMPROVEMENT

S. VIZIREANU^a, A. LAZEA STOYANOVA^a, M. FILIPESCU^a,
D.-L. CURSARU^{b*}, GH. DINESCU^a

^aNational Institute for Lasers, Plasma and Radiation Physics, Romania

^bPetroleum-Gas University of Ploiești, Romania

Carbon nanowalls coatings were synthesized by radiofrequency plasma beam. The tribological behavior of the carbon nanowalls coatings in the presence of low sulfur diesel fuel was investigated by high frequency reciprocating rig (HFRR) test. The CNWs layers before friction tests were investigated by scanning electron microscopy (SEM), atomic force microscopy (AFM) and Raman spectroscopy while the wear on the steel balls was investigated by optical microscopy of the HRRT apparatus and the wear track on the steel disk was investigated by SEM, AFM and profilometry. Our study presents the potential of CNWs as lubricating factor and the results are compared with other carbon base materials such as graphite and carbon nanotubes. It has been found that CNWs layers exhibit a lubricating potential for the rubbed surfaces in the presence of low sulfur diesel fuels. Tribological analyses of various carbon materials reveal that friction coefficient of carbon nanowalls is close to the values obtained for graphite.

(Received July 25, 2013; Accepted August 26, 2013)

Keywords: Carbon nanowalls; Nanosheet; Vertically graphene; Anti-wear coatings; Lubricity tests

1. Introduction

In the recent years, many studies have been done in order to reduce harmful compounds from diesel fuel, especially with sulfur, to diminish the polluting effects of sulfur containing gases such SO₂ from the exhaust pipe of the cars. One of the most efficient industrial processes, used for the removal of the sulfur compounds from diesel fuels, is catalytic hydrodesulphurization (HDS) [1]. Unfortunately, the effect of the deep sulfur removal consists in a poor lubrication quality of diesel fuels that could cause problems to the engine and to the injection system working with. In the last years, because of public awareness concerning the environmental protection, EU Parliament imposed few regulations which require that all EU members should replace some vol. % of the diesel fuel with alternative biofuels such as biodiesel. In fact, biodiesel offers a way to reduce harmful emissions and more than that, it was proven in numerous scientific researches, that few vol. % of biodiesel can restore the lubricity of low sulfur diesel fuel [2-10].

Amorphous and nano-crystalline carbon films possess special tribological proprieties [11]. It is well known [12-13] that the carbon based materials which contain a great extent of sp² bond, as graphite-like and fullerenes-like structures [14], present a low friction coefficient, low wear and a good corrosion resistance. Usually these materials present self-lubricating behaviors. Utilization of carbon nanomaterials in tribological applications is a new research topic, different carbon allotropes such as diamond-like, graphite-like and the newer fullerene-like and nanotubes have been studied for their special physical and chemical properties [15-21]. Lately, an intensive effort for the enhancement of the mechanical and tribological characteristics of materials based on graphene multilayer composites and graphene platelets for applications [22-24], was made.

In such conditions, Carbon Nanowalls (CNWs), as carbon nano-materials, made of few overlaid/superposed graphene layers [25], could be a possible candidate for the tribological

* Corresponding author: dianapetre@yahoo.com,

applications. These nano-materials are composed of quasi-two dimensional lamellar structures dominated by large amount of sp^2 carbonic phase. These multilayer graphene flakes are interconnected as honeycomb networks that covering the substrate. In a previous study, we developed a reproducible method for obtaining [26] this kind of nano-materials based on graphene onto various substrates type.

In this paper, we focused on lubrication properties of solid nanowalls coatings synthesized by radiofrequency plasma beam deposition on metallic surfaces which are in direct contact with the low sulfur diesel fuel. To our knowledge this is the first study in which the lubricity properties of CNWs are tested. A comparison between lubricity properties of steel disk coated with CNWs layers of various characteristics is done. Moreover, tribological characterization of admixing and dispersing CNW and other carbon allotropes (i.e. graphite, single wall carbon nanotubes-SWNTs and multi wall carbon nanotubes- MWNTs) in the diesel fuel was investigated.

2. Materials and experimental methods

Our study presents briefly the synthesis process and characterization of CNWs with an emphasis on the tribological properties of CNWs. The tribological investigations consist in lubricity tests by HFRR procedure of various sizes CNWs deposited on steel disks and detailed comparison between CNWs and other carbonaceous materials results is made.

2.1. Materials

2.1.1. Preparation of CNWs coatings

CNWs were synthesized by using low pressure RF plasma jet in $Ar/H_2/C_2H_2$ gas mixture. Detailed description of the synthesis method can be found in our previous studies [26-28]. In this study we used polished regular stainless steel and AISI-E 52100/535A99 steel disk as substrates for growing CNWs. A pre-treatment, for substrates cleaning and activation, was performed, first in Ar/H_2 (1050/25 sccm) plasma, at 300 W radiofrequency power, 700 C, for 5 minutes.

After cleaning and activation, the CNWs coatings were deposited in the plasma jet generated in $Ar/H_2/C_2H_2$ mixture, using different flow ratios without using any catalyst. As we have previously shown [28], CNWs layers with different characteristics (length, height, surface density, and graphitic content) can be obtained by varying the Ar flows mass flow rate during the synthesis procedure and keeping the other deposition parameters constant. In this study, we have used four Ar flows (700, 1050, 1400 and 1600 sccm), while the other parameters were: H_2/C_2H_2 ratio was 25/1 sccm, RF power 300 W, substrates temperature 700°C, 30 minutes deposition time. During coating, the pressure values were determined by the mass flow rates and the pumping speed, and were in the range of 0.8 to 1.4 mbar. For an easy identification, the samples were labeled after the used Ar flow values with names: CNW700, CNW1050, CNW 1400 and CNW1600, respectively.

This method allowed us to obtain uniform CNWs coatings onto the steel disks [28], the cross section SEM investigations (not shown here) revealed that CNW700 has about 1 μm , CNW1050 about 3 μm , and CNW1600 has about 7 μm .

2.1.2. The characteristics of CNWs coatings

Prior to the tribological measurements, the CNWs layers were investigated by SEM (FEI S Inspect working at 20 kV), AFM and Raman (Bruker FT Raman RFS/100S and Horiba Jobin Yvon T64000 spectrophotometers). After the lubricity tests, the wear on the steel balls was investigated by optical microscopy of the HRRT apparatus and the wear track on the steel disk was investigated by SEM, AFM and profilometry. The AFM investigation was done with Park Systems XE-100 instrument (maximum horizontal scan range of $50\mu m \times 50\mu m$ and maximum vertical movement of 12 μm), and the measurements were done in tapping mode. A P6 stylus profilometer

from KLA Tencor Corporation (up to 150 mm scan length and 1 mm Z range) was used to investigate the two and three-dimensional profile and morphology of the wear track. Profilometry data was operated by MountainsMap Software (Digital Surf) trial version.

For example, the morphology (obtained by SEM) of the CNW1400 sample deposited on stainless steel is presented in Figure 1a. The CNW coating consists of few layers of graphene as interconnected network of lamellar flakes oriented perpendicular on the substrate. Concerning the topography of the samples, CNW1400 can be observed in the AFM image from Figure 1b. The mean roughness of the CNW sample is about 129 nm.

The structure and chemical bonding of carbon atoms in the CNWs were discussed elsewhere. They were investigated by TEM, SAED [26-29] and XPS [29]. We showed that an individual CNW consist in thin carbon foils (10-30 nm thickness) composed from stacked nanographitic domains (about 5 nm in size) [27, 30] slightly aligned with their c-axis perpendicular on foil surface. The amount of sp^2 hybridized carbon bond type coming from their multilayer graphene-like structure exceeds the few percents of sp^3 hybridization phase which occur manly at the interconnections, at the “in-wall-boundary” regions [31] and defects-like [32] in the graphitic network of the nanowalls.

The SEM investigations carried out for all our CNWs coated samples point out the same trend of morphology variation with the Ar flow rate, as discussed in the reference [28]: the size of CNWs increases and the number of individual CNWs on substrate decreases by increasing the Ar mass flow rate.

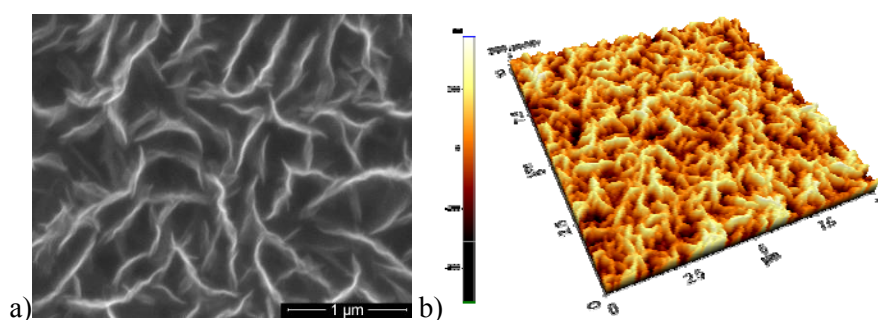


Fig.1. a) Morphology and b) topography of CNW1400 coated disk sample

The graphitic nature of CNW700, CNW1050, CNW1400 grown on steel substrate, was revealed by Raman spectroscopy, at an excitation wavelength of 514 nm. In Figure 2 we can observe the over-layered Raman spectra of these samples, normalized to G band for an easier comparison. All spectra show a typical spectrum of multilayers graphene nanosheets, very similar to the defective graphite [33]. As we previously found on CNWs onto Si and Au substrates [28, 29] and the literature reported [33-35], the carbon nanowalls present the so-called D (at about 1350 cm^{-1}) and G (at ca 1585 cm^{-1}) bands and their combinational mode 2D (at ca 2700 cm^{-1}) and D+G (at 2930 cm^{-1}) bands that originated from double resonance mechanism. The presence of D and G bands, including their second order mode, demonstrate the graphitic-like nature of the material. These spectra sustained the existence of sp^2 phase signature of the nano-graphitic domains [33] in the obtained CNW coatings on a steel substrate. A more ordered graphitic phase was obtained in the case of CNWs synthesized at higher Ar low ratios. The increasing of the 2D intensities is a clear proof of the material quality improvement and of the graphitic phase quantity as well.

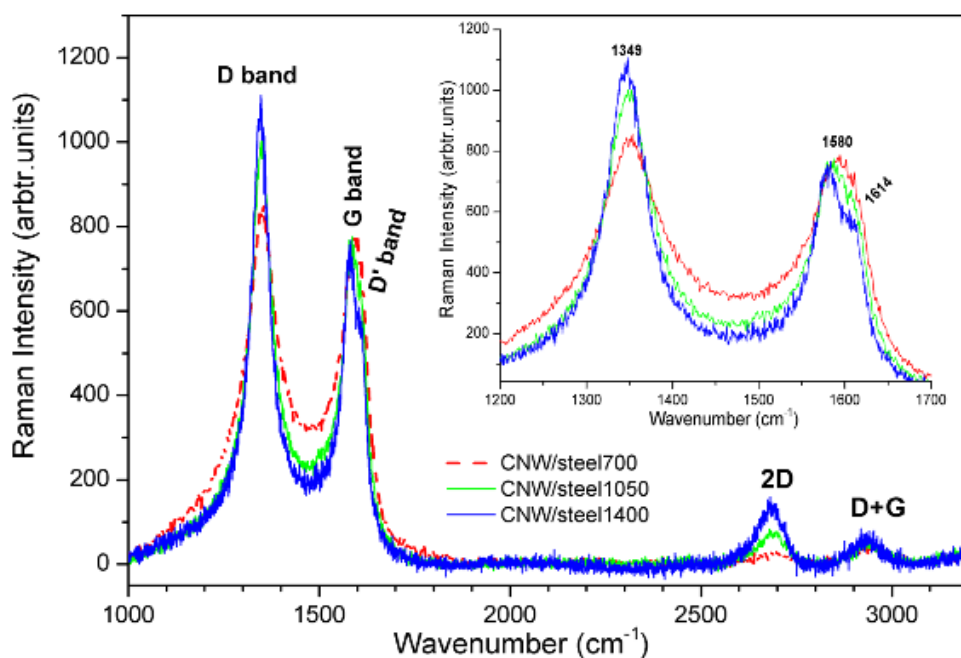


Fig. 2. Raman spectra (normalized to G peak) of CNW samples deposited on steel substrate

2.1.3. Diesel fuel

In order to study the application of carbon nanowalls as possible enhancers of lubricity of fuels, a low sulfur diesel fuel was chosen as lubrication fuel because of its poor lubrication properties. The physical characteristics of the chosen diesel fuel are depicted in table 1.

Table 1. Physical-chemical properties of low sulfur diesel fuel

Properties	Results	Methods
Density (25°C, kg/m ³)	826.2	ASTM D-1298
Sulfur (wt %)	0.0017	ASTM D-2622
Viscosity at 40°C, cSt	4.12	ASTM D-455
Cetane number	49.2	ASTM D-613
Cloud point, °C	-20.0	ASTM D-2500
<i>Distillation</i>	°C	ASTM D-86
IBP	185.8	
50%	248.2	
EP	365.9	
Hydrocarbon type	% vol	ASTM D-1319
Aromatics	28.8	
Olefins	1.9	
Saturates	69.3	
Lubricity WS1.4, μm	636	ASTM-D6079

2.2. Lubricity Tests

Conventionally, the lubricity of diesel fuels is investigated by High Frequency Reciprocating Rig (HFRR) tests, according to ASTM D-6079. The HFRR is a reciprocal friction and wear test system which rapidly enables repeatable assessment of the performance of fuels and

lubricants, particularly being suitable for wear-testing of lubricants and has the main advantage of using small quantities of lubricants.

The HFRR test consists in friction of an AISI-E 52100/535A99 steel ball (with a roughness of $R_a=0.050 \mu\text{m}$ and a hardness of RC 58-66) against an AISI-E 52100/535A99 disk (with 10 mm diameter and a roughness of $R_a=0.020 \mu\text{m}$ and a hardness of RC 76-79) in the presence of 2 ± 0.2 ml lubricant at a frequency of 50 ± 1 Hz, 1000 μm stroke, 200 ± 1 g load and $60 \pm 2^\circ\text{C}$ (according to ASTM D-6079). The relative humidity was sustained between 40 and 60%, while the ambient temperature was between 24 and 26°C . The indicator of lubricity is the diameter of the wear scar imprinted on the steel ball, and a high value of the wear scar diameter indicates a poor lubricity efficiency of the fuel. The quoted wear scars are corrected to give the WSD values at a pressure of 1.4 kPa (denoted WS1.4). According to international standards the maximum wear scar diameter allowed for diesel fuel is limited to $460 \mu\text{m}$.

3. Results and discussion

3.1. Comparison of lubrication parameters of uncoated and coated surfaces

3.1.1. Study of the wear track on uncoated and CNWs coated steel disks

In the SEM images from Figure 3a and b, we can observe the wear scars on steel disks, uncoated and coated with CNW1400 after ball sliding on their surface. As concerning the surface morphology at the bottom of the track wear it is seen, by comparing in Figures 3 c and d, that the case of coated disks the surface is smoother and without deep scratches. This is better observed in the AFM investigations.

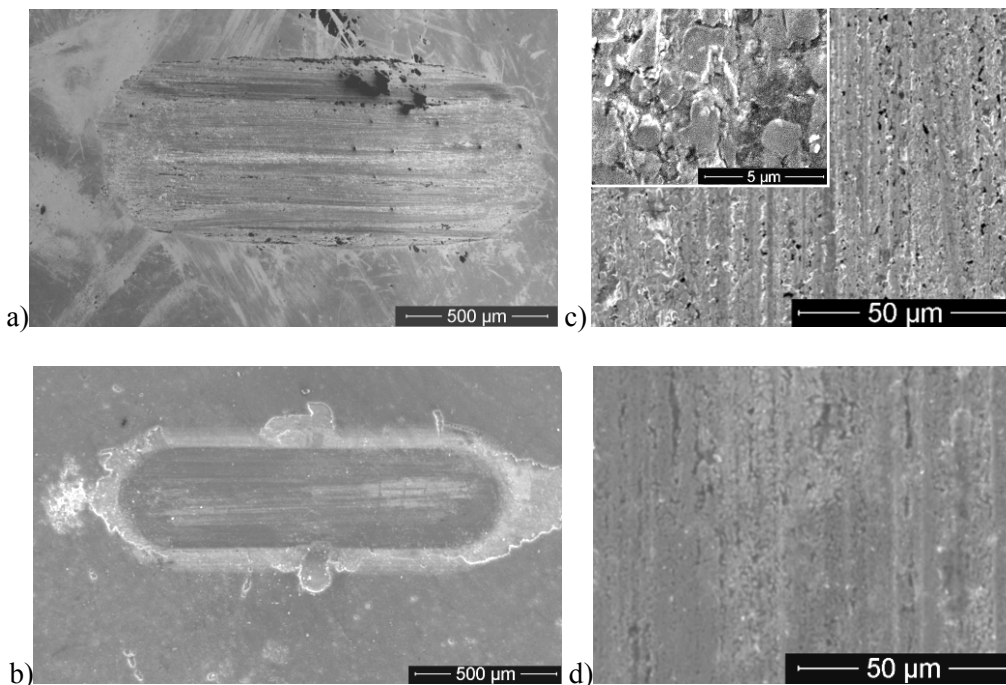


Fig. 3. SEM images of wear scar of a) uncoated and b) coated disk with CNW1400. The zoom SEM images in the wear track region of c) uncoated and d) coated CNW 1400 sample

The interfaces of the wear track are shown in Figure 4 a), where it is revealed (left part of the figure) that the CNWs architecture was removed from the wear track and possible tribo-film formations [11, 36], as we can be seen also in the SEM image from Figure 3d. Moreover, from Figure 4, we can observe that the CNWs were broken preferentially at the substrates level and pieces of CNWs were engaged with the fuel drop out of the wear trace. We can see some individual CNWs flakes on the top of CNWs coatings (point out by arrow in figure 4b). These flakes appear after the lubricity experiments and seem to be detached from the wear zone.

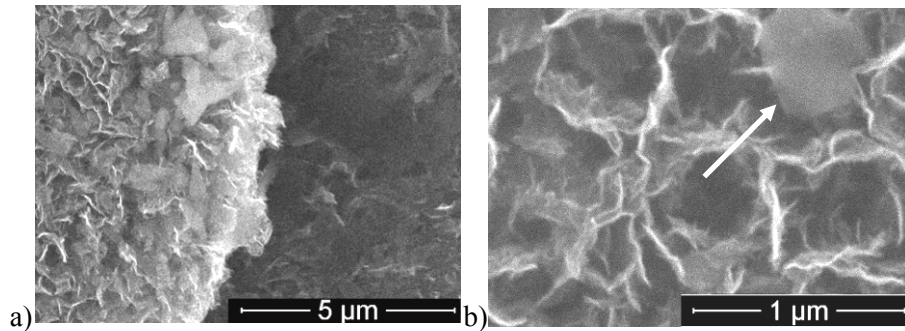


Fig.4. SEM images of a) border between the CNWs/wear interfaces and b) CNW layers near to wear

AFM investigations on the track wear region for benchmark steel disk (a) and CNW1400 coated disk (b), are presented in Figure 5. The scanned area was $40 \times 40 \mu\text{m}$, a close value to the maximum of scan area of the AFM device. The AFM images show the surface topography and indicate the roughness in the groove.

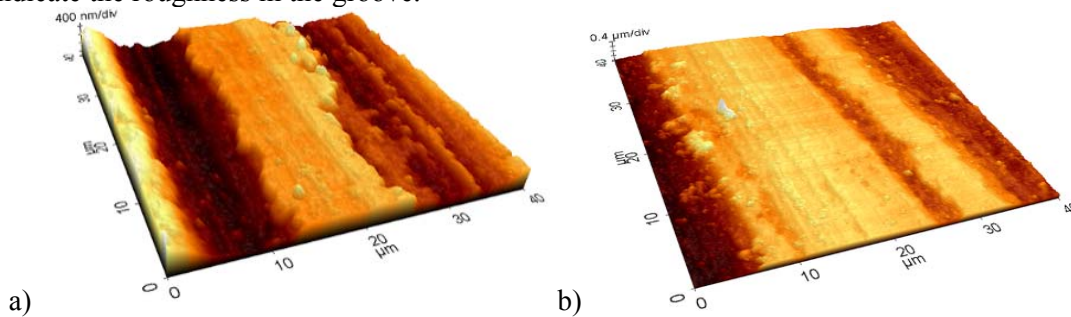


Fig.5. The topography in track wear region a) benchmark ($rms \sim 300 \text{ nm}$) and b) CNW1400 sample ($rms \sim 169 \text{ nm}$)

A decreasing of the roughness in the wear track of the steel disk after coated by CNW1400 is noticeable. However, the comparison of roughness values is only considered as indicative, because the roughness depends strongly on the position in the wear track, and the accidental presence of debris and broken CNWs architectures.

More complete evaluations of the wear track were obtained through profilometry. The 3D images obtained by surface scan (about $1 \times 2 \text{ mm}$) in the region of the wear track are presented in Figure 6a, for uncoated and coated disks. Figure 6b presents a zoom of median region of a wear profile.

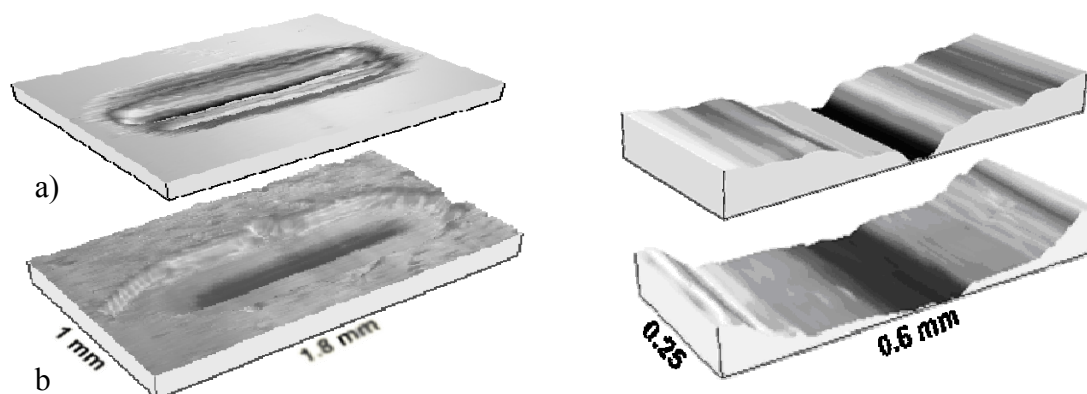


Fig. 6. 3D morphologies of wear profile onto a) benchmark steel disk, b) CNW1400 samples; and a zoom in the wear profile for c) benchmark (top) and d) CNW1400 samples (bottom). after tribological experiments

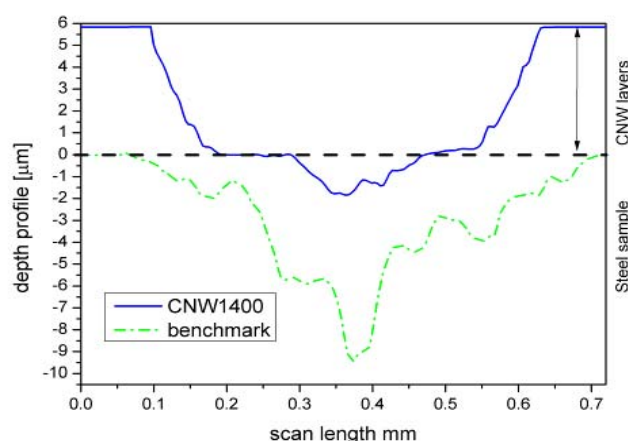


Fig. 7. 2D profile of wear track of uncoated and coated steel disk after the lubricity test

In Figure 7 we can observe a 2D depth profile of the wear track on benchmark steel disk and CNW1400 coated disk samples. The profiles were aligned with respect to the uncoated surface level, figured by a dotted line. The part of the profile above zero accounts for the thickness of deposited CNW layer. It is noticed that, after the sliding test, the wear track of the uncoated steel disk is much deeper (9.4 mm) compared to CNW1400 coated disk (1.8 mm deepness, excluding the CNW thickness).

3.1.2. Dependence of lubrication properties upon CNW characteristics

In order to study the influence of the CNWs material characteristics on the lubrication properties we have performed lubrication experiments with coatings consisting of CNWs of different sizes and graphitic content. As we have reported before [28, 29] and also mentioned here (section 2.1.2 from SEM and Raman investigations), the size and graphitic content of the individual nanostructures increase in the sample series, from CNW700 to CNW1600.

Fig. 8 (a-d) present three-dimensional profiles of the wear track of steel disks coated with CNWs layers, obtained at an increasing Ar mass flow rate. The depth profiles of the wear tracks of

samples are shown in Fig.8e. All depth profiles use the same baseline, of the level of the steel substrate, allowing an easy comparison of wear on the steel disks.

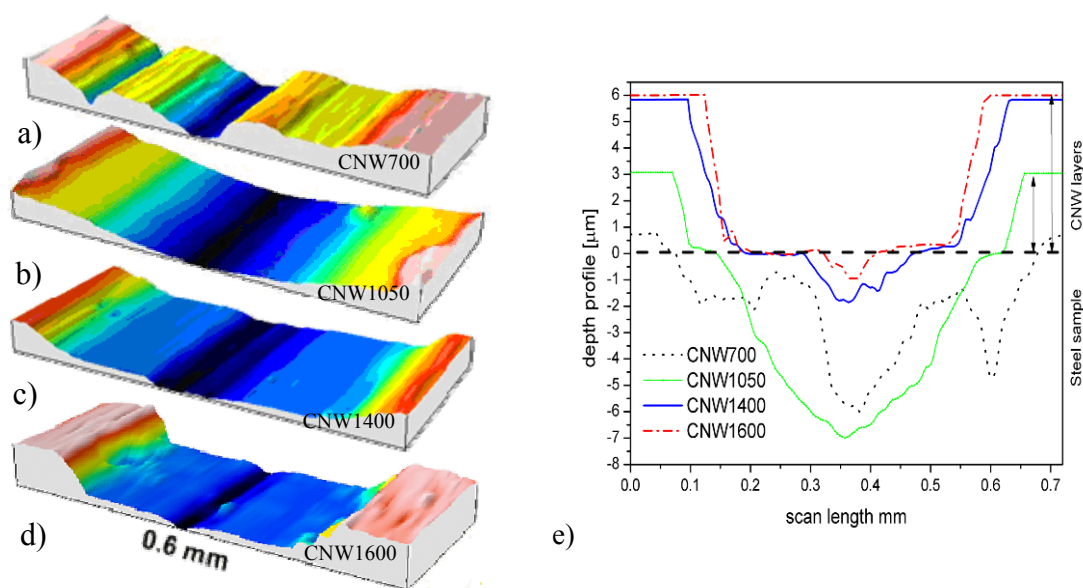


Fig. 8. 3D profile of the wear track a) CNW700, b)CNW1050, c) CNW1400, CNW1600 samples and e) The depth profiles of the wear track of samples CNW700, CNW1050, CNW1400 and CNW1600

The depth profiles of the wear tracks of the steel disks decrease from $\sim 7 \mu\text{m}$ (sample CNW1050) to $\sim 1.2 \mu\text{m}$ (sample CNW1600). An exception to this behavior is seen for the sample CNW700, where some abrasive traces and a wider wear track is observed. Additionally, the W-shape profile of the wear track of the sample CNW700 is similar to shape profile of the uncoated sample, this indicate that layer obtained for a lower Ar flow (i.e. CNW700) have a poor lubricity. However, the depths of all the wear tracks of the CNWs coated disks (included CNW700) are smaller than the depth of uncoated steel disk, see Fig. 7. The samples coated with CNWs deposited at higher Ar flow have smooth, similar to each other -shape profiles indicating a better lubricity. This increasing of lubricity correlates with the increasing amount of graphitic phase; thus an easier sliding can be induced which in turn results in a low wear track and friction coefficients, as we will further show by ball analysis.

3.2. Study of the lubrication properties of CNW by HFRR; results on ball

The lubricity tests performed for all four samples with CNWs coatings were compared with the result of the lubricity test for low sulfur diesel fuel without any additives.

The evolution of the wear scar diameters for low sulfur diesel fuel with different CNWs samples are observed in figure 9.

The results observed for CNWs 700 coating are not promising, the wear scar diameter being superior to the wear scar diameter corresponding to the non additivated diesel fuel.

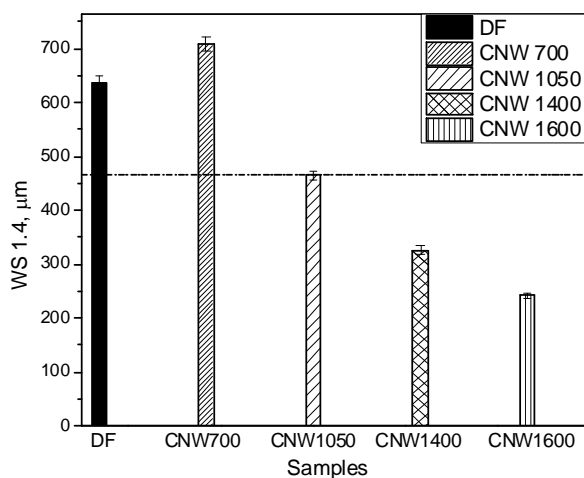


Fig. 9. Wear scar diameters for low sulfur diesel fuel with different CNW samples

However, by coating the surface of the metallic disks with CNWs 1050, 1400 or 1600, the results are notable; the wear scar diameters decrease under the value imposed by the standards.

In Figure 4 are presented the friction coefficients observed for different type of CNWs coatings. The evolution of the friction coefficients follows a similar tendency as wear scar diameters, inferior tribological properties were associated to CNWs 700 coating while the most promising coating was CNWs 1600. These interesting results are completed by the values for the thickness of the lubricant layer during lubrication tests. The smallest value of the thickness of the lubricant layer was recorded for CNWs 700 respectively 13% while for CNWs 1050 was 49%, 82% for CNWs 1400 and 86% for CNWs 1600.

The sample with the worst lubrication and tribological properties has the smallest value for the thickness of the lubricant layer, probably, during the friction the layer becomes thinner and the friction is taking place in the boundary lubrication domain and a metal-metal friction might occur.

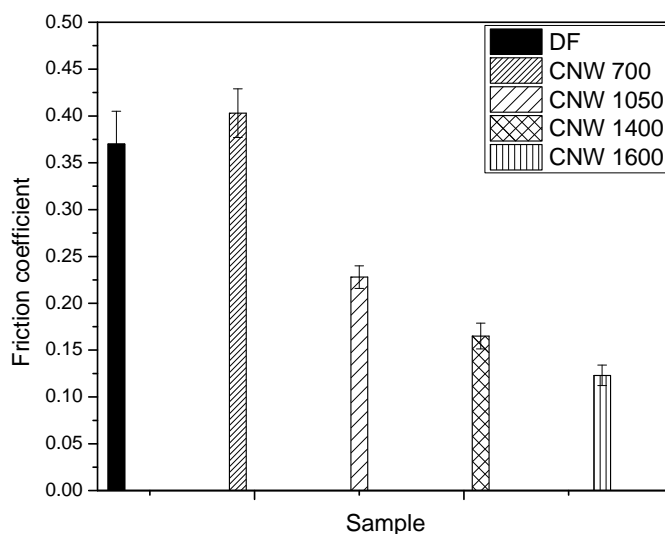


Fig. 10. Friction coefficients for low sulfur diesel fuel with different CNW samples

3.3. Comparisons of lubrication properties of CNWs with other carbonic materials

In order to perform these experiments, 0.25 wt% CNWs flakes have been dispersed into diesel fuel by ultrasonication for 30 min and the results were compared with those recorded for similar concentration of graphite, or SWNTs, or MWNTs dispersed in diesel fuel.

HFRR results in Figure 11 show the wear scar diameter (WS1.4) as a function of lubrication in the presence of different carbon materials.

It is evident that all carbon compounds improve the lubricity of the low sulfur diesel fuel and the best results were achieved for graphite, while the highest value for the wear scar diameter, thus the poorer lubricity, was recorded for diesel fuel additivated with MWNTs. Unfortunately, by dispersion of 0.25 wt % of these carbonaceous materials, the wear scar diameter has not sufficiently diminished in order to achieve the upper limit for the lubricity of commercial diesel fuels.

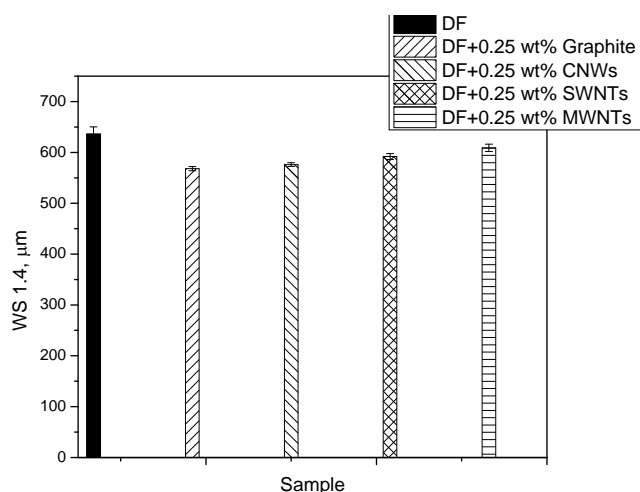


Fig.11. Wear scar diameters for low sulfur diesel fuel with different carbonaceous materials

Parallel to the evaluation of the wear scar diameter it was recorded, in Figure 12, the evolution of the friction coefficients as a function of addition of different carbonaceous materials to diesel fuel.

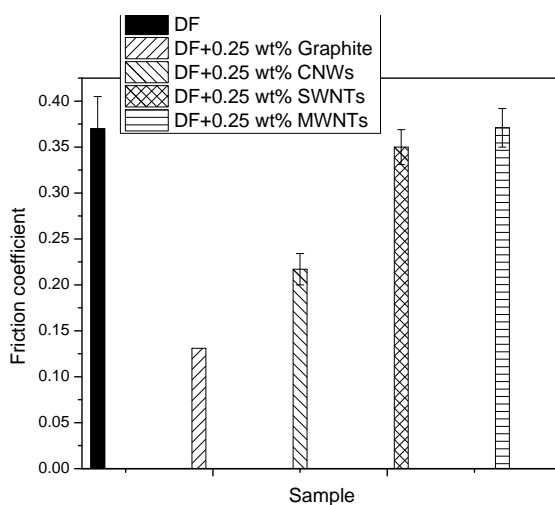


Fig. 12. Friction coefficients for low sulfur diesel fuel with different carbonaceous materials.

The evolution of the friction coefficients follows similar trend as the wear scar diameter, the highest value of the friction coefficient being observed for diesel fuel with MWNTs while the smallest friction coefficient was recorded for diesel fuel with graphite. Actually, these results are in agreement with others who associate very attractive tribological properties for graphite [16, 17].

The main draw back of this assessment is the low potential of the carbonaceous materials to remain stable in suspension. After 72 hours from the dispersing step, the suspension became unstable and it was observed a tendency of all carbonaceous materials to drop to the bottom of the flask. The aim for further experiments is utilization of room temperature ionic liquids or functionalized carbon materials to stabilize the suspension.

4. Conclusions

Carbonaceous materials, such as graphite, SWNTs, MWNTs, and CNWs, reveal attractive lubrication properties however this study reveal that CNWs exhibit excellent lubrication and tribological behavior. This fact was indicated by low wear scar diameters and low friction coefficients.

When the steel disk was coated with CNWs the lubricity properties were improved compared to uncoated disk. Changes on the CNWs characteristics indicate a decreasing of depth profile in the wear scare with increasing of the graphitic phase. This might be explained by the creation of a thin protective layer at the steel surface, acting as an important factor for the increase of tribological performance.

Tribological analyses of various carbon materials reveal that carbon nanowalls friction coefficient is close to the values obtained for graphite.

Deposition of CNWs materials on disks seems to be more efficient from lubrication and friction points of view, the wear scar diameter and the friction coefficient observed for CNWs coating were inferior to the values obtained for CNWs flakes dispersed in diesel fuel.

In conclusion the CNWs obtained by RF plasma demonstrate their potential in tribological applications.

Acknowledgements

The authors are gratefully acknowledging to I. Baltog from National Institute for Materials Physics, Magurele for the Raman investigations and to Attila Sirovita from KLA Tencor Company for the profilometer measurements.

The authors are grateful acknowledges the financial support from the Romanian Ministry of Education and Research under the contract PN-II-RU-TE_228 (No. 92/2010) and contract PN-II-PCCA-140/2012.

References

- [1] E. Rodriguez-Castellon, A. Jimenez-Lopez, D. Eliche-Quesada, *Fuel* **87**, 1195 (2008)
- [2] http://ec.europa.eu/energy/res/legislation/doc/biofuels/en_final.pdf
- [3] A. Keskin, M. Gürü, D. Altiparmak, *Bioresource Technology* **99**, 6434 (2008)
- [4] M.G. Kulkarni, A.K. Dalai, N.N. Bakhshi, *Bioresource Technology* **98**, 2027 (2007)
- [5] J. Hancsok, M. Bubalik, A. Beck, J. Baladincz, *Chem. Eng. Research and Design* **86**, 793 (2008)
- [6] D.C. Drown, K. Harper, E.A. Frame, *J Am Oil Chem Soc* **78**, 579 (2001)
- [7] J.W. Munson, P.B. Hertz, A.K. Dalai, M.J. Reaney, *SAE*, 1999-01-3590
- [8] X. Lang, A.K. Dalai, *Tribotest Journal* **8**, 131 (2001)
- [9] G. Anastopoulos, E. Lois et al., *Energy Fuels* **15**, 106 (2001)
- [10] G. Anastopoulos, F. Zannikos et al., *Tribology International* **34**, 749 (2001)
- [11] P. K. Chu, L. Li, *Materials Chemistry and Physics* **96**, 253 (2006)
- [12] B. Bhushan, *Diamond and Related Materials- Invited Review* **8**, 1985 (1999)
- [13] A. Grill, *Wear* **168**, 143 (1993)

- [14] P. Wang, X. Wang, B. Zhang, W. Liu, *Thin Solid Films* **518**, 5938 (2010)
- [15] U.D. Schwartz, O. Zwörner, P. Köster, R. Wiesendanger, *Physical Review B* **56**, 6987 (1997)
- [16] C. Donnet, A. Grill, *Surface and Coatings Technology*, **94-95**, 456 (1997)
- [17] A. Erdemir, O.L. Eryilmaz, G. Fenske, *Journal of Vacuum Science and Technology* **18** (4), 1987 (2000)
- [18] T. Cao, F. Wei, Y. Yang, L. Huang, X. Zhao, W. Cao, *Langmuir* **18**, 5186 (2002)
- [19] D.L. Cursaru, C. Andronescu, C. Pirvu, R. Rîpeanu, *Wear* **290-291**, 133 (2012)
- [20] D.L. Cursaru, I. Ramadan, C. Tanasescu, R. Rîpeanu, *Digest Journal of Nanomaterials and Biostructures* **8** (2), 805 (2013)
- [21] D.L. Cursaru, D. Enescu, D. Ciuparu, *Revista de Chimie* **62** (8), 792
- [22] J. Zhang, Y. Yu, D. Huang, *Solid State Sciences* **12**, 1183e1187 (2010)
- [23] J. Lin, L. Wang, G. Chen, *Tribol Lett* **41**, 209 (2011)
- [24] V. Eswaraiah, V. Sankaranarayanan, S. Ramaprabhu, *ACS Appl. Mater. Interfaces* **3**, 4421 (2011)
- [25] A. Malesevic, R. Vitchev, K. Schouteden, A. Volodin, L. Zhang, G. Van Tendeloo, A. Vanhulsel, C. Van Haesendonck, *Nanotechnology* **19**, 305406 (2008)
- [26] S. Vizireanu, L. Nistor, M. Haupt, V. Katzenmaier, C. Oehr, G. Dinescu, *Plasma Processes and Polymers* **5**, 263 (2008)
- [27] S. Vizireanu, S.D. Stoica, C. Luculescu, L.C. Nistor, B. Mitu, G. Dinescu, *Plasma Sources Science and Technology* **19**, 034016 (2010)
- [28] S. Vizireanu, B. Mitu, C.R. Luculescu, L.C. Nistor, G. Dinescu, *Surface and Coatings Technology*, doi:10.1016/j.surfcoat.2011.07.09 (2011)
- [29] Z. González, S. Vizireanu, G. Dinescu, C. Blanco, R. Santamaría, *Nano Energy*, <http://dx.doi.org/10.1016/j.nanoen.2012.07.003> (2012)
- [30] K. Kobayashi, M. Tanimura, H. Nakai, A. Yoshimura, H. Yoshimura, K. Kojima, M. Tachibana, *J. Appl. Phys.* **101**, 094306 (2007)
- [31] N. Jiang, H. X. Wang, H. Zhang, H. Sasaoka, K. Nishimura, *J. Mater. Chem.* **20**, 5070 (2010)
- [32] N. G. Shang, P. Papakonstantinou, M. McMullan, M. Chu, A. Stamboulis, A. Potenza, S. S. Dhesi, H. Marchetto, *Adv. Funct. Mater.* **18**, 3506 (2008)
- [33] Z.H. Ni, H.M. Fan, X. F. Fan, H.M. Wang, Z. Sheng, Y.P. Feng, Y.H. Wu, Z.X. Shen, *J. Raman Spectroscop.* **38**, 1449 (2007)
- [34] S. Kurita, A. Yoshimura, H. Kawamoto, T. Uchida, K. Kojima, M. Tachibana, P. Molina-Morales, H. Nakai, *J. Appl. Phys.* **97**, 10320 (2005)
- [35] H. G. Jain, H. Karacuban, D.Krix, H.-W. Becker, H. Nienhaus, V. Buck, *Carbon* **49**, 4987 (2011)
- [36] S. Gayathri, N.Kumar, R.Krishnan, T.R.Ravindran, S.Dash, A.K.Tyagi, B. Raj, M.Sridharan, *Tribology International* **53**, 87 (2012)